Available online at www.sciencedirect.com

SciVerse ScienceDirect

Ceramics International 39 (2013) 1169–1182

CERAMICS INTERNATIONAL

www.elsevier.com/locate/ceramint

Tribological behaviour of powder metallurgy-processed aluminium hybrid composites with the addition of graphite solid lubricant

P. Ravindran[a,*,1], K. Manisekar[b], R. Narayanasamy[c], P. Narayanasamy[d]

[a]Department of Mechanical Engineering, St. Mother Theresa Engineering College, Thoothukudi 628102, Tamil Nadu, India
[b]Centre for Manufacturing Sciences, National Engineering College, Kovilpatti 628 503. Tamil Nadu, India
[c]Department of Production Engineering, National Institute of Technology, Tiruchirappalli 620015, Tamil Nadu, India
[d]Department of Mechanical Engineering, Renganayagi Varatharaj College of Engineering, Sivakasi 626128, Tamil Nadu, India

Received 17 April 2012; received in revised form 12 July 2012; accepted 12 July 2012
Available online 24 July 2012

Abstract

The tribological behaviour of powder metallurgy-processed Al 2024–5 wt% SiC–x wt% graphite (x=0, 5, and 10) hybrid composites was investigated using a pin-on-disc equipment. An orthogonal array, the signal-to-noise ratio and analysis of variance were employed to study the optimal testing parameters using Taguchi design of experiments. The analysis showed that the wear loss increased with increasing sliding distance and load but was reduced with increased graphite content. The coefficient of friction increased with increasing applied load and sliding speed. The composites with 5 wt% graphite had the lowest wear loss and coefficients of friction because of the self-lubricating effect of graphite. Conversely, due to the effect of the softness of graphite, there was an increase in wear loss and the coefficient of friction in composites with 10 wt% graphite content. The morphology of the worn-out surfaces and wear debris was examined to understand the wear mechanisms. The wear mechanism is dictated by the formation of both a delamination layer and mechanically mixed layer (MML). The overall results indicated that aluminium ceramic composites can be considered as an outstanding material where high strength and wear-resistant components are of major importance, particularly in the aerospace and automotive engineering sectors.

Keywords: B. Composite; C. Friction; C. Wear resistance; D. SiC

1. Introduction

In recent years, aluminium metal matrix composites (AMMCs) have been used in the aerospace, aircraft and automotive industries, particularly for lightweight cylinder liners because AMMCs have many advantages, including higher strength, higher wear resistance, higher thermal conductivity and lower coefficient of friction. [1,3,7,9]. An improvement in the tribological properties of AMMCs has been successfully attained by introducing ceramic particles, such as SiC, B_4C, Al_2O_3, TiC and AlN. Both the mechanical strength and wear resistance of composites increase with the addition of SiC ceramic particulates to the aluminium matrix alloy. These aluminium-based ceramic composites require not only good mechanical strength and high wear resistance but also self-lubrication properties [2,3]. The use of a single reinforcement in an aluminium matrix may sometimes compromise its physical properties [4]. However, the consequent increase in SiC content in composites makes machining difficult [4,5]. Thus, it is essential to identify ways to retain the advantageous influence of SiC while simultaneously addressing the problems of machining SiC-reinforced composites.

*Corresponding author. Tel.: +91 9842160709, +91 461 2328915.
E-mail addresses: energyravindran@gmail.com, sweetravindran@yahoo.com (P. Ravindran).
[1]Present address: 57/D, Vannar 2nd street, Melashunmugapuraam, Thoothukudi 628003, Tamil Nadu, India.

0272-8842/$ - see front matter © 2012 Elsevier Ltd and Techna Group S.r.l. All rights reserved.
http://dx.doi.org/10.1016/j.ceramint.2012.07.041

Graphite particulates are well suited to this application, and their addition improves the machinability and wear resistance of Al–SiC composites. Al–SiC composites reinforced with graphite particulates are known as Al–SiC–Gr hybrid composites [6,7].

A number of studies have reported on the dry sliding wear behaviour of aluminium composites reinforced with various ceramic particles [1–14]. An investigation of machining Al–Gr composites by Krisnamurthy et al. showed a considerable reduction of cutting forces, which has been attributed to a possible reduction of friction due to the solid lubrication of Gr particulates [8]. Thus, graphite can be advantageously used as a second reinforcement to overcome the problem of machining brittle SiC-reinforced composites [6–8]. The combined effect of aluminium alloy reinforced with ceramics and graphite imparts good wear properties to the composite [7–9]. Mahdavi and Akhlaghi investigated the effect of SiC content on the processing, compaction behaviour, and properties of Al6061/SiC/Gr hybrid composites using an in-situ powder metallurgy (IPM) technique [6]. Basavarajappa et al. reported on the influence of sliding speed on the dry sliding wear behaviour and subsurface deformation of hybrid metal matrix composites using a liquid metallurgy technique [9]. TedGuo and Tsao reported the tribological behaviour of self-lubricating aluminium/SiC/graphite hybrid composites synthesised by the semi-solid powder-densification method [10]. There are many articles focused on the synthesis of silicon carbide/Gr aluminium composites using different routes [2,5,11–17], such as stir-casting, squeeze casting, in-situ, semi-solid powder densification and spray co-deposition. However, the powder metallurgy route is rarely found in the literature. The powder metallurgy route to manufacturing metal matrix composites offers advantages compared with ingot metallurgy, stir-casting, and squeeze casting because of its low manufacturing temperature, which avoids strong interfacial reactions, minimising undesired reactions between the matrix and the reinforcement. An additional advantage of powder metallurgy is the uniformity in the reinforcement distribution. This uniformity improves not only the structural properties but also the mechanical strength as well as imparts high wear resistance. Based on literature sources, studies on the tribological behaviour of hybrid composite are very limited. However, most of the reported research focuses on the effect of either one or two factors on the dry sliding wear behaviour of hybrid composites. There is no systematic study reported thus far that investigates the various factors that influence the tribological behaviour of hybrid composites. The principal objective of this investigation was to fabricate hybrid aluminium matrix composites by powder metallurgy and evaluate their basic tribological properties. Furthermore, an attempt was made to study the effect of applied load, sliding speed and sliding distance on the friction and wear behaviour of the hybrid composites using Taguchi design of experiments. Analysis of variance was employed to find the percentage of influence of various factors and their interactions. Furthermore, the SEM morphology of the worn surfaces, wear debris and the EDX of worn surfaces were analysed to understand the wear mechanisms.

2. Experimental setup and procedures

2.1. Specimen preparation

The composites were fabricated through the P/M process route. Aluminium 2024 was used as the matrix material in the present investigation, and details of its composition are given in Table 1. This matrix was chosen because it provides an excellent combination of strength and damage tolerance at elevated and cryogenic temperatures. To perform the study, three types of composites were prepared

(i) Al/5 wt% of SiC composite.
(ii) Al/5 wt% of SiC/5 wt% of Gr hybrid composite.
(iii) Al/5 wt% of SiC/10 wt% of Gr hybrid composite.

Fig. 1 shows typical SEM micrographs of the as-received aluminium, SiC and graphite powder particles. SEM observations confirmed that the mean diameter of Al powder (Fig. 1a) was approximately 30 μm, and the mean diameters of both the SiC and graphite particulates were approximately 50 μm (Figs. 1b and c). Table 2 provides details about the SiC and graphite particulates, which were used as reinforcements. Table 3 lists details about the hybrid composites. Powders used in this study were elemental powders of aluminium, copper, magnesium, manganese, iron, silicon, chromium, zinc, silicon carbide and graphite. All of the metal powders were supplied by M/s Metal Powder Company Ltd., Madurai, Tamil Nadu, India. Silicon carbide was obtained from M/s Grindwell Norton, Bangalore, India. Al 2024 was prepared by mechanical alloying. First, the elemental powders were dried at 110 °C in an oven for 1 h. Mixing of the powder was performed in a planetary tumbler mixer using stainless steel balls with a diameter of 8 mm and a ball to powder weight ratio of 10:1, with a mixing time up to

Table 1
Chemical composition of the matrix alloy.

Element	Cu	Mg	Fe	Mn	Si	Cr	Zn	Al
Content%	4.0	1.8	0.5	0.25	0.5	0.25	0.2	Balance

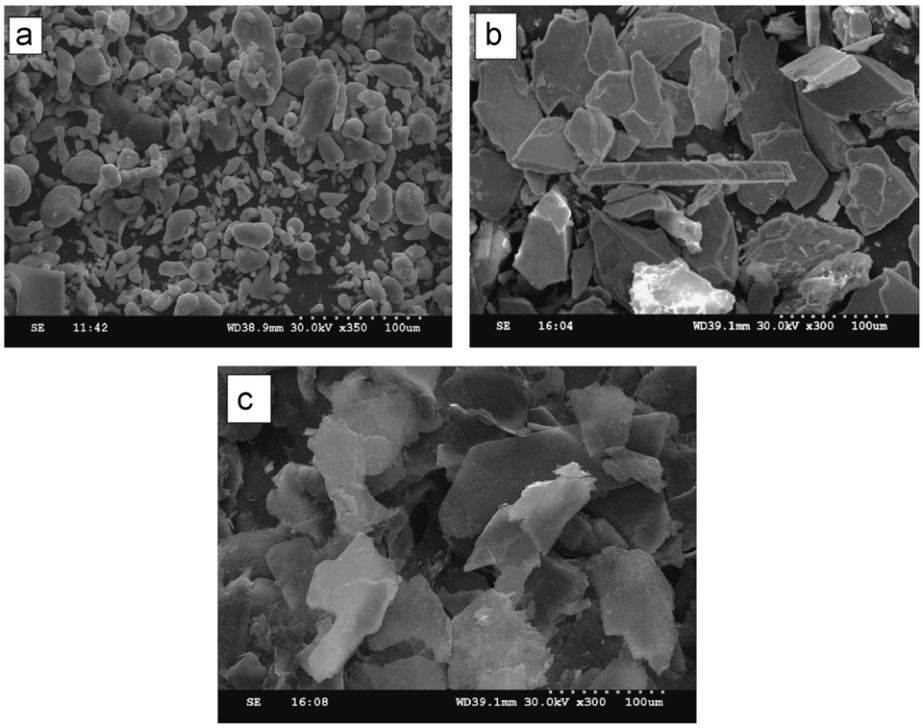

Fig. 1. SEM micrographs of as-received (a) Aluminium powders (b) SiC particles and (c) Gr particles.

Table 2
Details of reinforcements.

Reinforcement	Grain size (μm)	Density(g/cm^3)
SiC	43–53	3.22
Gr	43–60	2.09–2.23

Table 3
Mechanical properties of the samples.

Sample no.	Composition (wt%)	Density (g/cm^3)	Hardness (BHN)
1	Al–5% SiC	2.89	55
2	Al–5%SiC–5% Gr	2.84	53
3	Al–5% SiC–10% Gr	2.82	51

6 h. Mixing was performed at 50 rpm using toluene to prevent oxidation. Then, different weight fractions of graphite particles (0, 5, and 10 wt%) were mixed in the tumbler mixer with the matrix powder. The mixed powders were pressed in a uniaxial press at 845 MPa to form green compacts [10]. Before each run, die wall lubrication was performed manually using zinc stearate. The green compacts were sintered at a closely regulated temperature of 530 °C for 60 min, as suggested by Yamagushi et al. [18]. The sintered composites were solution treated at 540 °C in a muffle furnace for 120 min and water quenched; then, they were naturally aged for 72 h. The wear specimens were manufactured with a diameter of 8 mm and a height of 30 mm. The ends of the specimens were sequentially polished with abrasive paper of grades 600, 800 and 1000. The density of the composite specimens was determined using a high precision digital electronic weighing balance with an accuracy of 0.0001 mg using Archimedes' principle. The hardness of the composites was evaluated using a Brinell hardness tester. Table 3 shows the mechanical properties of the samples. Details of the as-produced powder mixtures and microstructures of the sintered composites were given in previous studies [1].

2.2. Wear test

Dry sliding wear tests were performed in accordance with the ASTM G99-05 (reapproved 2010) test standards [19] for the pin-on-disc equipment (Ducom, model No: ED-201, Bangalore, India). The counter disc material was EN31 steel. Prior to testing, the pins and disc surface were cleaned with acetone. All of the tests were performed on hybrid composite pins of various compositions with applied loads of 10 and 20 N. A varying sliding distance of 1000 or 3000 m was employed, with sliding speeds of 1 m/s and 2 m/s. After each test, the specimen and counter face disc were cleaned with organic solvents to remove traces of composite. The pin was weighed before and after testing to an accuracy of 0.1 mg to determine the amount of wear loss. The coefficient of friction was determined from the applied normal load and the tangential load obtained from the strain gauges. Each test was repeated six times, and the average results were taken.

2.3. Experimental design

The Taguchi method is a powerful experimental tool that offers a simple, efficient and systematic approach to determine optimal parameters. Compared with the conventional approach to experimentation, this method considerably reduces the number of experiments that are required to model response functions. Traditional experimentation involves one-factor-at-a-time experiments, where one variable is changed, while the remaining variables are held constant. The major shortcoming of this strategy is that it fails to consider any possible interactions between the parameters. An interaction is the failure of one factor to produce the same effect on the response at different levels of another factor. It is also impossible to study all of the factors and determine their main effects (i.e., the individual effects) in a single experiment. The Taguchi technique overcomes all of these drawbacks. The main output is the average value of the response function at a particular level of a parameter. The effect of a factor level is the deviation it causes from the overall mean response. The Taguchi method is devised for process optimisation and identification of optimal combinations of factors for given responses [20]. The experimental observations are transformed into a signal-to-noise (S/N) ratio. There are several S/N ratios available depending on the type of characteristics. The three categories of S/N ratios used are smaller-the-better, higher-the-better and nominal-the-best. The S/N ratio for the minimum wear loss and coefficient of friction are under the smaller-the-better characteristic.

The S/N ratio can be calculated as a logarithmic transformation of the loss function, as shown below

$$S/N = -10 \log 1/n\left(\sum y^2\right)$$

where 'n' is the number of observations, and y is the observed data.

The four process parameters were studied at three levels, as shown in Table 4. The experiments were performed under the conditions given in Table 5. Mean-response graphs were plotted using a Minitab-16 software, and the percentage of contribution of testing parameters was determined by ANOVA analysis [21].

Table 4
Levels for various control factors.

Control factors	Units	Level I	Level II	Level III
A: Gr reinforcement	wt%	0	5	10
B: load	N	10	15	20
C: sliding distance	m	1000	2000	3000
D: sliding speed	m/s	1	1.5	2

3. Results and discussion

3.1. ANOVA and the effects of factors

To obtain a concrete visualisation of the impact of various factors A (Gr reinforcement wt%), B (load), C

Table 5
Experimental design using L27 (2^{13}) orthogonal array.

L27 (2^{13})	A	B	C	D	Wear loss (gm)	S/N ratio (db)	Friction co-efficient	S/N ratio (db)
1	0	10	1000	1.0	0.0095	40.4455	0.153	16.30617
2	0	10	2000	1.5	0.0110	39.1721	0.174	15.18902
3	0	10	3000	2.0	0.0118	38.5624	0.182	14.79857
4	0	15	1000	1.5	0.0108	39.3315	0.192	14.33398
5	0	15	2000	2.0	0.0134	37.4579	0.206	13.72266
6	0	15	3000	1.0	0.0229	32.8033	0.162	15.8097
7	0	20	1000	2.0	0.0098	40.1755	0.216	13.31092
8	0	20	2000	1.0	0.0163	35.7562	0.191	14.37933
9	0	20	3000	1.5	0.0182	34.7986	0.202	13.89297
10	5	10	1000	1.5	0.0042	47.5350	0.158	16.02686
11	5	10	2000	2.0	0.0048	46.3752	0.171	15.34008
12	5	10	3000	1.0	0.0153	36.3062	0.144	16.83275
13	5	15	1000	2.0	0.0048	46.3752	0.159	15.97206
14	5	15	2000	1.0	0.0129	37.7882	0.151	16.42046
15	5	15	3000	1.5	0.0154	36.2496	0.154	16.24959
16	5	20	1000	1.0	0.0078	42.1581	0.198	14.0667
17	5	20	2000	1.5	0.0121	38.3443	0.211	13.51435
18	5	20	3000	2.0	0.0140	37.0774	0.216	13.31092
19	10	10	1000	2.0	0.0022	53.1515	0.172	15.28943
20	10	10	2000	1.0	0.0119	38.4891	0.166	15.59784
21	10	10	3000	1.5	0.0121	38.3443	0.176	15.08975
22	10	15	1000	1.0	0.0086	41.3100	0.181	14.84643
23	10	15	2000	1.5	0.0092	40.7242	0.184	14.70364
24	10	15	3000	2.0	0.0148	36.5948	0.187	14.56317
25	10	20	1000	1.5	0.0084	41.5144	0.193	14.28885
26	10	20	2000	2.0	0.0126	37.9926	0.214	13.39172
27	10	20	3000	1.0	0.0185	34.6566	0.228	12.8413

(sliding distance), D (sliding speed) and their interactions, it was desirable to develop an analysis of variance (ANOVA) table to determine the order of significant factors and their interactions. This analysis was undertaken for a level of confidence of significance of 5%. Tables 6 and 7 show the results of the ANOVA of hybrid composites in terms of the wear and friction coefficients in this investigation. Table 6 shows that sliding distance ($p=57.12\%$) had the great influence on wear loss. Gr reinforcement wt% ($p=11.23\%$), load ($p=13.78\%$), and sliding velocity ($p=12.43\%$) showed less significant contributions to the wear loss, but the interactions had no significant contribution to the wear loss.

Similarly, Table 7 shows that load ($p=61.47\%$) had a large influence on the friction coefficient. Gr reinforcement wt% ($p=8.84\%$) and sliding velocity ($p=8.86\%$) showed less significant contributions to the friction coefficient. The interaction of A × B ($p=7.93\%$) showed a relatively less significant contribution to the friction coefficient, but the remaining sliding distance and other interactions did not make a significant contribution to the friction coefficient. Thus, the sliding distance was found to be the most influential testing parameter for controlling wear loss. However, the applied load was found to be the most influential parameter in controlling the coefficient of friction. The Gr % of reinforcement had a moderate influence (11.23% and 8.84) in both cases.

3.2. Influence of testing parameters on wear loss

Fig. 2 shows a graph of the main effects of the influence of the various testing parameters on both the wear loss and coefficient of friction of the composites. In the main effect plot, if the line for a particular parameter is near horizontal, then the parameter has no significant effect. In contrast, a parameter for which the line has the highest inclination has the most significant effect. It was clear from the main effect plot that parameter C (sliding distance) was the most significant parameter, while parameters A (reinforcement%), B (load) and D (sliding speed) had relatively less influence. The increase in the sliding distance caused more asperity-to-asperity contact time and resulted in an increased real area of contact, which in turn led to the formation of wear debris and increased wear of the composites. Wear loss increased with an increase of the applied load and sliding distance, which indicated more removal of material from the surface. In addition, wear

Table 6
Analysis of variance for wear loss, using adjusted SS for tests.

Source	Degrees of freedom	Sum of squares	Adjusted sum of squares	Adjusted mean of squares	*F*-ratio	*P*-value	Percentage of contribution
A	2	0.0000646	0.0000646	0.0000323	16.97	0.003	11.23
B	2	0.0000793	0.0000793	0.0000397	20.84	0.002	13.78
C	2	0.0003285	0.0003285	0.0001643	86.31	0.000	57.12
D	2	0.0000715	0.0000715	0.0000358	18.80	0.003	12.43
A × B	4	0.0000103	0.0000103	0.0000026	1.35	0.353	1.79
A × C	4	0.0000030	0.0000030	0.0000008	0.40	0.805	0.52
B × C	4	0.0000066	0.0000066	0.0000016	0.87	0.535	1.15
Error	6	0.0000114	0.0000114	0.0000019			1.98
Total	26	0.0005753					100

S=0.00137961, R-Sq=98.02% and R-Sq (adj)=91.40%.

Table 7
Analysis of variance for friction coefficient, using adjusted SS for tests.

Source	Degrees of freedom	Sum of squares	Adjusted Sum of squares	Adjusted Mean of squares	F-ratio	P-value	Percentage of contribution
A	2	0.0012336	0.0012336	0.0006168	5.16	0.050	8.84
B	2	0.0085696	0.0085696	0.0042848	35.85	0.000	61.47
C	2	0.0001202	0.0001202	0.0000601	0.50	0.628	0.86
D	2	0.0012349	0.0012349	0.0006174	5.17	0.050	8.86
A × B	4	0.0011062	0.0011062	0.0002766	2.31	0.172	7.93
A × C	4	0.0004036	0.0004036	0.0001009	0.84	0.545	2.90
B × C	4	0.0005569	0.0005569	0.0001392	1.16	0.412	4.00
Error	6	0.0007171	0.0007171	0.0001195			5.14
Total	26	0.0139420					

S=0.0109325, R-Sq=94.86% and R-Sq (adj)=77.71%.

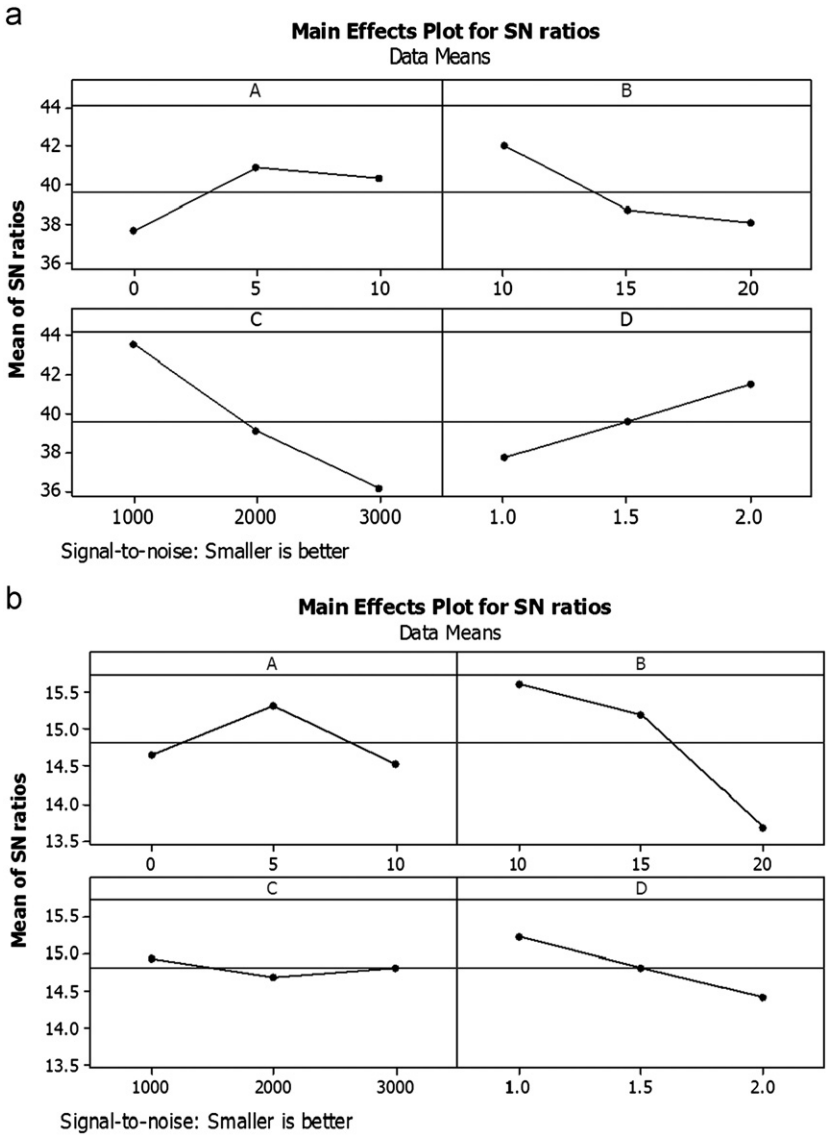

Fig. 2. Main effects plot of factors (a) Wear of Al–SiC–Gr hybrid composites and (b) friction coefficient of Al–SiC–Gr hybrid composites.

loss decreased with an increase in the sliding speed due to the formation of a graphite-rich layer on the worn surfaces, thus reducing wear by covering more area of contact. At higher loads, the composite with 5% showed better wear resistance compared to other conditions (i.e., 0% and 10%).

3.3. Influence of testing parameters on the coefficient of friction

Fig. 3 shows the mean-response graphs for the influence of the testing parameters on the coefficient of friction. Applied load was the most significant factor influencing the coefficient of friction of the composite because parameter B had the highest inclination, while the sliding speed and reinforcement% had only slight effects. However, the friction remained almost invariant with sliding distance for all composites. The increase in the applied load significantly increased the coefficient of friction of the composites because at lower loads, the graphite film was found to be more stable than at higher loads, as the film was destroyed at a faster rate with an increase in the load. The coefficient of friction decreased as the weight fraction increased up to 5 vol% and further increased with increasing weight fraction. This result is due to the presence of graphite in the aluminium matrix, which acts as a solid lubricant material on the surface and results in the formation of a solid lubricant-rich film on the tribosurface, thereby reducing the friction by preventing metal-to-metal contact on the sliding surface. When the wt% of graphite was above 5%, the friction showed an increasing trend due to fracturing of the oxide layer within the surface, which weakens worn surfaces. Abrasion through the decohesion of sliding surfaces causes contact between the composites and counter face. As a result, the coefficient of friction increased.

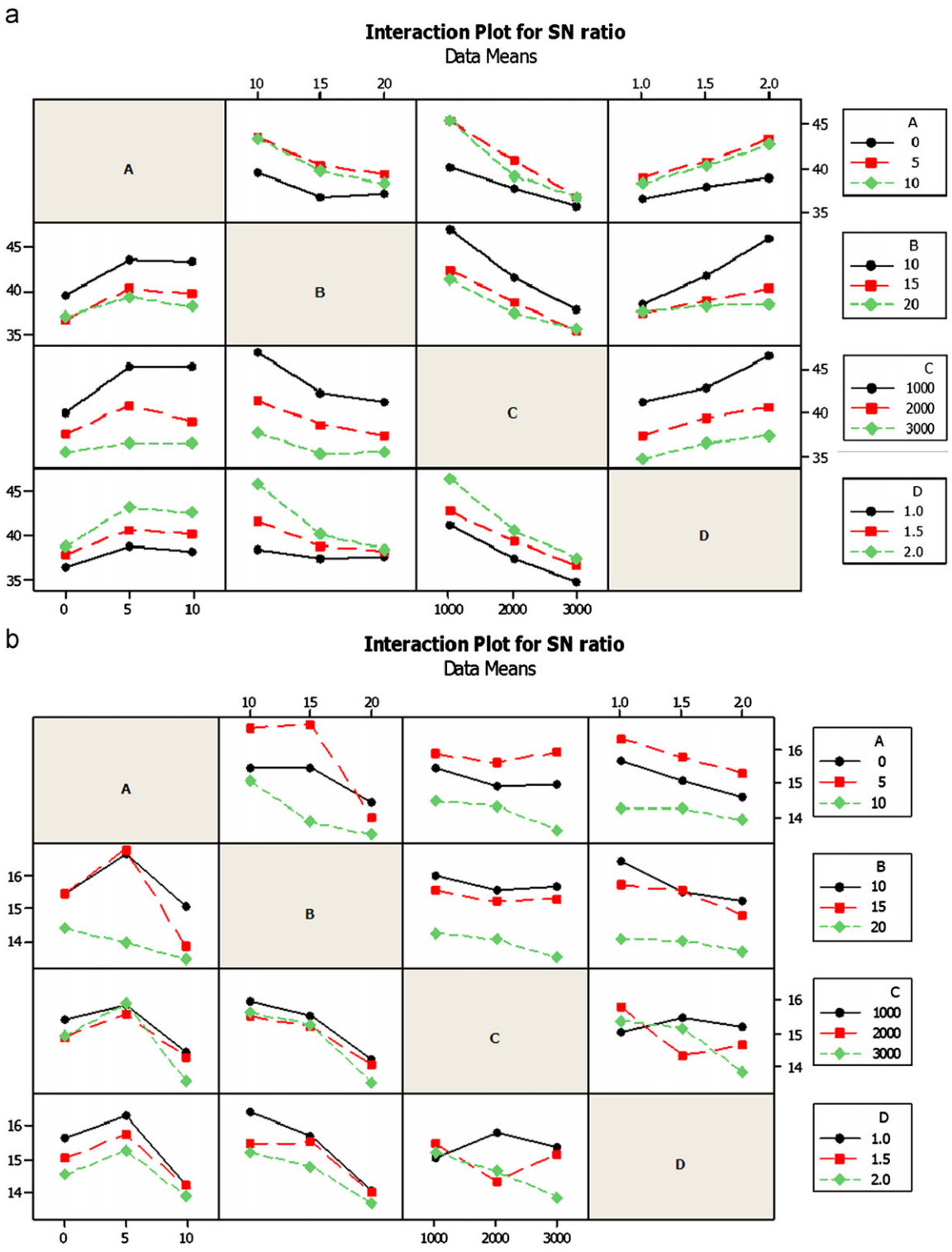

Fig. 3. Interaction plots for (a) wear loss and (b) Co efficient of friction (μ).

3.4. Analysing and evaluating the results of the experiments using the Taguchi method

The essential criterion in the Taguchi method for analysing experimental data are signal/noise ratio (S/N). In this study, the S/N ratio should have a maximum value to obtain optimum testing conditions, according to the Taguchi method. The S/N response tables of the wear and friction coefficient for the prepared hybrid composites are presented in Table 8. The response table shows the average of the selected characteristics for each level of the factors. The response table includes ranks based on Delta statistics, which compare the relative magnitude of effects. The Delta statistic is the highest average for each factor minus the

Table 8
Response table for signal-to-noise ratios: smaller is better.

Level	Wear response				Friction coefficient response			
	A	B	C	D	A	B	C	D
1	37.61	42.04	43.56	37.75	14.64	15.61	14.94	15.23
2	40.91	38.74	39.12	39.56	15.30	15.18	14.70	14.81
3	40.31	38.05	36.15	41.53	14.51	13.67	14.82	14.41
Delta	3.30	3.99	7.40	3.78	0.79	1.94	0.24	0.82
Rank	4	2	1	3	3	1	4	2

Table 9
Results of confirmation tests.

Level	Initial parameter combination	Optimal parameter combination	
		Prediction	Experimentation
	A3B3C3D3	A2B1C1D3	
Wear (gm)	0.0162	0.00287	0.0027
SN ratio (dB)	35.8097	50.8423	51.3727
Improvement of S/N ratio: 15.563			
	A3B3C3D3	A2B1C1D1	
Friction (μ)	0.0162	0.1466	0.144
SN ratio (dB)	12.4317	16.6773	16.8328
Improvement of S/N ratio: 4.4011			

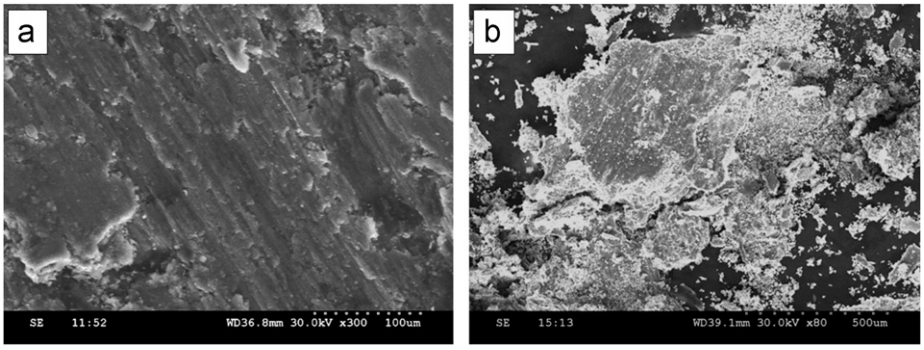

Fig. 4. SEM morphologies of Al–5% SiC composite at applied load of 20 N. (a) Worn surface and (b) wear debris.

lowest average for the same. Ranks are assigned based on Delta values; rank 1 is assigned to the highest Delta value, rank 2 to the second highest Delta value, and so on [22]. The optimum testing conditions were a Gr reinforcement of 5%, load of 10 N, sliding distance of 1000 m and sliding velocity of 2 m/s for the best wear resistance and a Gr reinforcement of 5%, load of 10 N, sliding distance of 1000 m and sliding speed of 1 m/s for the best friction values.

3.5. Confirmation experiment

The confirmation experiment is highly recommended by Taguchi to verify experimental conclusions. After the optimum conditions were determined, the confirmation experiment was performed with a combination of the optimum levels to compare the results with the predicted performance [22]. Table 9 shows the comparison of the estimated wear loss with the actual wear loss using the optimal parameters. It should be noted that there was good agreement between the estimated and observed results. The increase in S/N ratio from the initial testing parameters to the optimal testing parameters was 15.563 dB and 4.4011 dB, which meant that wear loss was reduced by approximately 56.54% and by 64.6% for the coefficient of friction. This finding indicates that the model constructed in this work can be effectively used to predict both the wear behaviour and friction coefficient of the composites.

3.6. Wear mechanism

Fig. 4(a–b) shows typical SEM micrographs of worn surfaces and wear debris morphology of the Al–5%SiC

composite at 20 N. The worn surface of the Al–5% SiC composite (Fig. 4a) clearly exhibited the presence of deep permanent grooves and fracture of the oxide layer, which may have caused the increased wear loss. The wear debris particles observed in Fig. 4b were large and shaped like thin sheets. This morphology shows that the Al–5% SiC composite had undergone significant severe plastic deformation, causing fracture of the SiC reinforcements. However, the worn surfaces of the other two composites (Fig. 5a and Fig. 6a) exhibited finer grooves and slight plastic deformation at the edges of the grooves. The surfaces also appeared to be smooth because of the graphite reinforcement content. The worn surface and wear debris morphology of the Al5% SiC–10%Gr composite is shown in Fig. 5(a–b). It is clear from Fig.5b and Fig.6b that the wear debris from the Al/SiC/Gr hybrid composites was smaller than the debris from the Al/SiC composite because the graphite particles scattered in the aluminium matrix can minimise the mean size of the wear particles. However, the wear debris of the hybrid composite consisted of a combination of fine and coarse powders with irregular shapes. As shown in Fig. 5b and Fig. 6b, the composite with 10% graphite had larger strip debris than the composite with 5% graphite because fracture of the reinforcement particles predominates over the effect of the solid lubricant. These wear mechanisms are characterised by the formation of grooves, which are produced by the ploughing action of hard asperities on the counter disc and hardened worn debris [20,21]. The increased temperature on the contact surface during the wear test is an important influential factor that determines the wear mechanism [22,23]. The temperature on the worn surfaces of both the Al–5% SiC and Al–5% SiC–10% Gr composites increased faster than that of the Al–5% SiC–5% Gr composites due to the larger coefficient of friction at the surface, which is evident from Fig. 3. Moreover, the friction coefficients of the Al–5% SiC–5% Gr composites were lower than that of the Al–5% SiC–10% Gr composite (refer Table 5). These parameters contribute to a slower temperature rise during the wear test, which led to reduced adhesion between interfaces in this composite [24]. However, the wear feature size in the worn surface was smaller because of the increased amount of graphite self-lubrication.

Fig. 7a and b shows the mechanically mixed layer on the worn surface of the Al–5% SiC–10% Gr and Al–5% SiC–5% Gr hybrid composites. Fig. 7a shows the loose particles at the worn surface, with mostly oxide particles of the aluminium matrix, indicating that severe deformation of the worn-out surface. In contrast, Fig. 7b shows very small size microcrystals of graphite particles, with smaller amounts of oxide particles at the worn surface. Additionally, these loose particles were tightly packed among themselves and formed an adherent film over the contact surfaces. This eventually led to a reduction of plastic deformation of the pin surface of the Al–5% SiC–5% Gr hybrid composite. As a result, the increase in temperature was partially reduced. The fine graphite grains were mixed with the other wear debris, and then, a smooth Gr-rich tribolayer was formed on the worn surface.

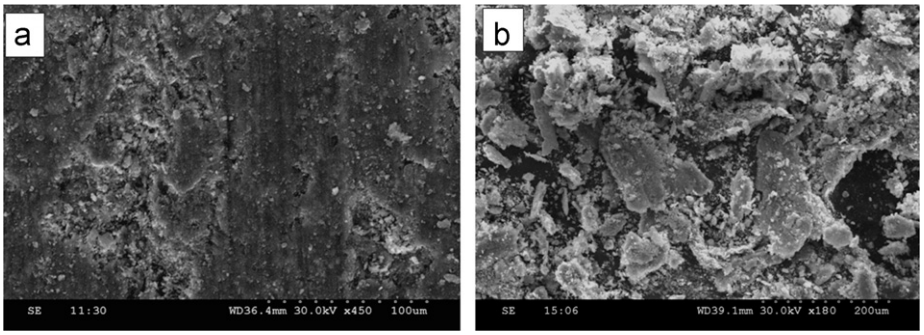

Fig. 5. SEM morphologies of Al–5% SiC–10% Gr composite at applied load of 20 N (a) worn surface and (b) wear debris.

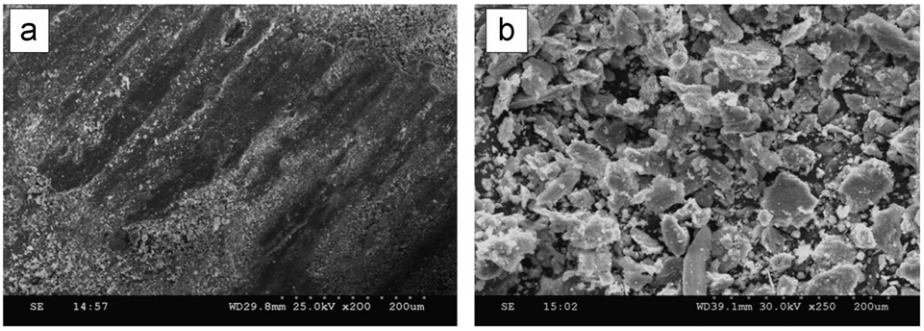

Fig. 6. SEM morphologies of the worn surface of Al–5% SiC–5% Gr composite at applied load of 20 N (a) worn surface and (b) wear debris.

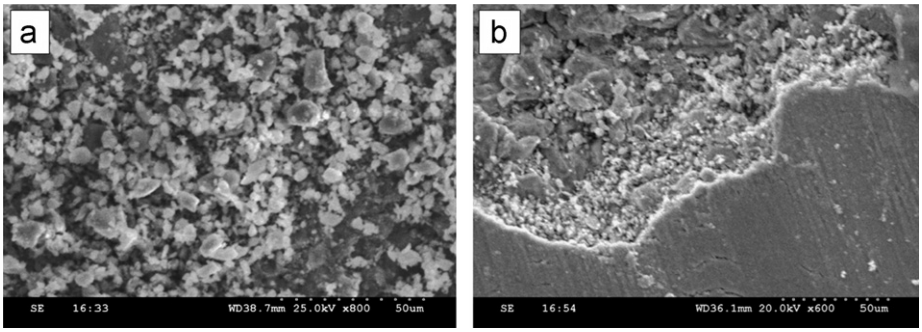

Fig. 7. SEM image of mixed layer (a) Al–5% SiC–10% Gr composite at applied load of 20 N and (b) Al–5% SiC–5% Gr composite at applied load of 20 N.

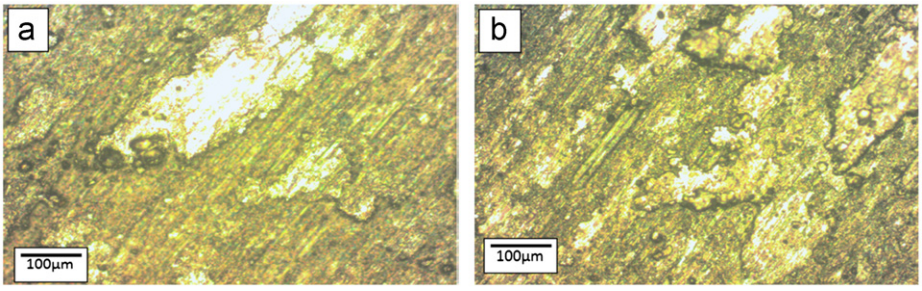

Fig. 8. Optical micrographs of the worn surface of disc mated with Al–5% SiC composite with a speed of 1.5 m/s at (a) applied load of 10 N and (b) applied load of 20 N.

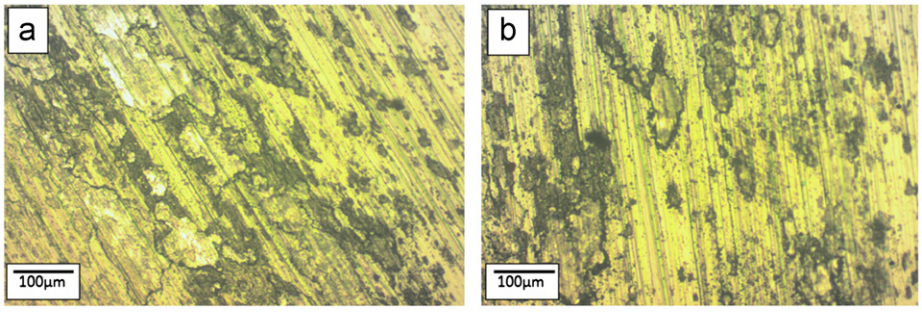

Fig. 9. Optical micrographs of the worn surface of disc mated with Al–5% SiC-10% composite with a speed of 1.5 m/s at (a) applied load of 10 N and (b) applied load of 20 N.

Therefore, the probability of severe wear in the Al–5% SiC–5% Gr composites is low, and abrasion and delamination are the dominant wear mechanisms [25,26].

3.7. EDX analysis

Energy dispersive X-ray (EDX) analyses of the worn surfaces of the composites were performed under dry wear conditions. In all EDX results of the hybrid composites, the presence of a small intensity oxygen peak was noted, indicating that some oxide formation at the worn surface had occurred. During sliding of the composite on a steel counter surface (EN31), the combined action of temperature increase and environmental reaction can lead to oxide film formation at the contact surfaces [26]. A typical EDX spectrum of the worn surface of the Al–5% SiC composite at 20 N and 2 m/s is shown in Fig. 11a. The EDX of the worn surfaces showed a low intensity Si peak and a high intensity Al peak. The high intensity Al peak indicated plastic deformation of the Al–5% SiC composite during sliding. The EDX spectrum of the worn surface of the Al–5% SiC–10% Gr composite at 20 N and 2 m/s is shown in Fig. 11b. Compared with the EDX profile of the Al–5% SiC composite worn surface, clear C peaks could be observed. The low intensity of the C peak indicated that the graphite solid lubricant was ineffective at the contact surface and that a graphite film was not formed. The moderate intensity of the Si peak indicated that SiC particles were pulled from the Al matrix. The EDX spectrum of the worn surface of the Al–5% SiC–5% Gr composite at 20 N and 2 m/s is shown in Fig. 11c. The strong C peak and the low intensity of the Al peak (compared with the other two EDX profiles) confirmed the increased smearing of graphite particles at the contact surface. However, a noticeable Fe peak was also found because the steel counter surface material was abraded by

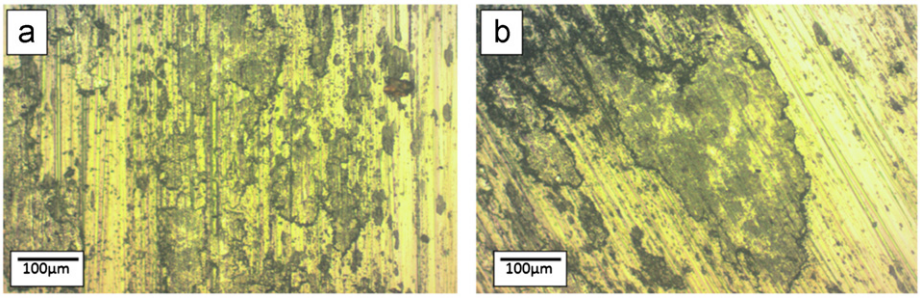

Fig. 10. Optical micrographs of the worn surface of disc mated with Al–5% SiC–5% Gr composite with a speed of 1.5 m/s at (a) applied load of 10 N and (b) applied load of 20 N.

the SiC particles. In all of the composite EDX results, the presence of a low-intensity oxygen peak was observed. This peak indicated that some oxide formation occurred at the worn surface of the mating parts. During the sliding of the composite against the steel counter surface, the joint action of the elevated temperature and the environmental reaction can cause the development of an oxide film on the contact surfaces [6,25,27].

3.8. Worn surface analysis of counter disc surface

The optical micrographs of the worn out surface of the disc against the composite pins are shown in Figs. 8–10. The surfaces were irregular, uneven and exhibited deep grooves while sliding against their counterpart pin. In Figs. 9 and 10, small degrees of graphitic films were detected on the worn surfaces. Fig. 10 shows a very thick graphitic film, indicating that very modest plastic deformation could have occurred during the sliding process.

4. Sliding wear behaviour

4.1. Effect of sliding distance on wear loss

Fig. 12 shows the wear loss as a function of the sliding distance. The wear rate of the Al/5SiC/10Gr composites was significantly lower than that of the Al/5SiC/5Gr and Al/5SiC composites. This effect was caused by the solid lubrication of graphite particles, which are released during sliding and form a tribolayer at the contact surfaces [2,28,29]. This constraint contributed to a slower temperature rise during the abrasive wear test, which led to reduced adhesion between interfaces in this composite [6,14,30]. However, the wear feature size in the worn surface was smaller because of the increased amount of graphite self-lubrication.

4.2. Effect of sliding velocity on wear loss

The variation of wear loss of the composites with sliding velocity is shown in Fig. 13. It was observed that an increase in sliding velocity resulted in decreased wear loss with all of the materials studied. However, at all of the sliding velocities studied, Al/5SiC/5Gr composites showed lower wear rates when compared with the other composites. A decrease in wear loss with an increase in sliding velocity is mainly caused by the solid lubrication of graphite particles, which are released during sliding and form a tribolayer at the contact surfaces [2,12,31]. With greater than 5% graphite reinforcement, the wear loss tends to increase. This tendency may be attributed to a decrease in the fracture toughness of the composite [2,12,30,31]. Under all studied sliding velocities, the Al/5SiC/5Gr composites demonstrated the lowest wear rates.

4.3. Effect of applied load on wear loss

The variation of wear loss with applied load at a constant sliding speed of 3 m/s and for a fixed sliding distance of 5000 m is shown in Fig. 14. It was observed that the wear loss of the hybrid composites increased gradually with an increase in load up to 15 N; after which, there was a steep rise in the wear loss. The increase in wear loss with increased load of all the materials studied can be attributed to the larger amount of plastic deformation and delamination wear at higher loads. Moreover, the composites with higher graphite content are more easily fractured or undergo matrix breakdown during sliding, which led to a higher wear loss with the Al–5% SiC–10% Gr composites. Under all of the studied loads and for a given reinforcement content, Al/5SiC/5Gr composites demonstrated the lowest wear loss.

4.4. Coefficient of friction with the effect of applied load

The coefficient of friction increased when the applied load was increased from 10 to 20 N, as shown in Fig. 15 (a and b). It is evident from this figure that the coefficients of friction of the Al/5SiC/5Gr and Al/5SiC/10Gr composites were less than those of the Al/5SiC composite. A higher coefficient of friction was exhibited by the Al–5% SiC composite under all of the load conditions. An increase in the coefficient of friction with an increase in the sliding distance can be mainly attributed to increased surface temperature [6,14,32]. Moreover, in the case of hybrid composites, the graphite was smeared on the contact surface, thereby reducing the metal-to-metal contact [33,34]. Due to the inherent self-lubrication properties

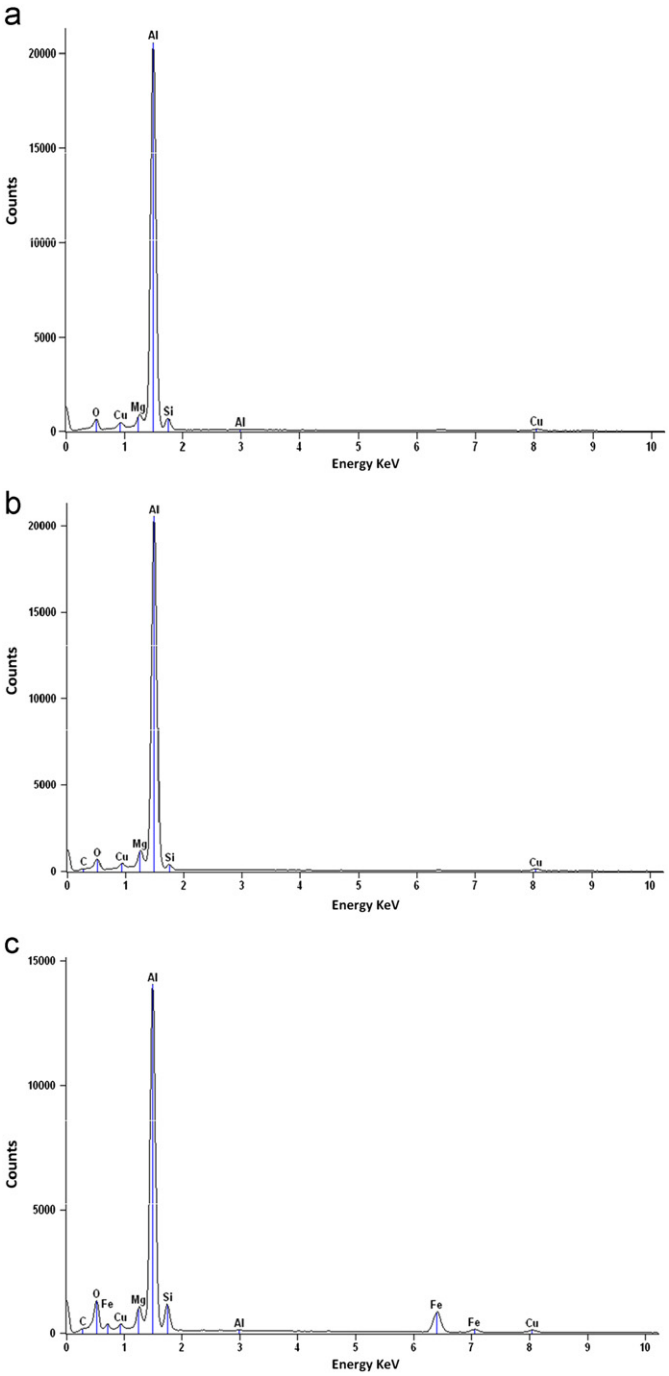

Fig. 11. EDX spectrum of worn surfaces at a sliding velocity of 2 m/s (a) Al–5% SiC composite (b) Al–5% SiC–10% Gr composite and (c) Al–5% SiC–5% Gr composite.

of the graphite film, the composites exhibited lower wear rates. This effect was predominant with the Al/5SiC/5Gr composite. A lower value of the coefficient of friction suggests less wear loss and higher values of the coefficient of friction signifies more wear loss [35]. A comparison of all of the figures clearly indicates that the coefficient of friction of the Al/5SiC/5Gr composite was the lowest among the other composite materials tested.

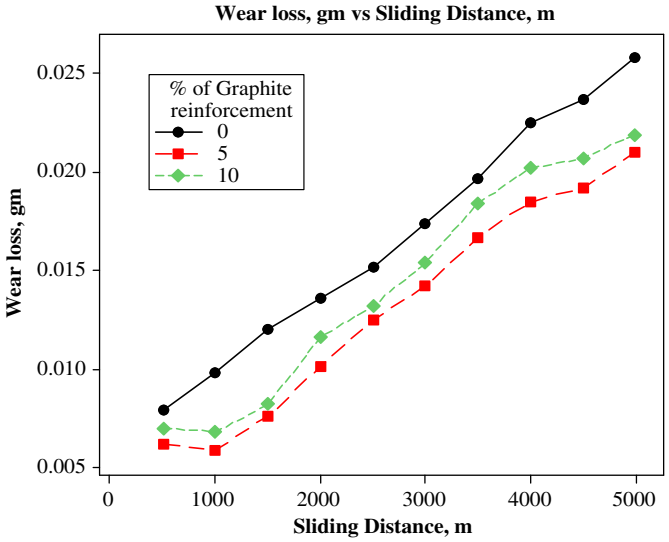

Fig. 12. Variation of wear loss against sliding distance at constant load of 15 N at 3 m/s.

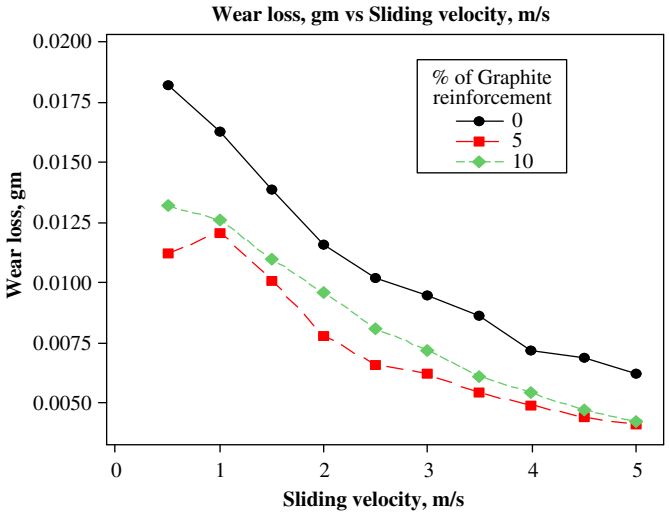

Fig. 13. Variation of wear loss against sliding velocity at constant load of 15 N for a constant sliding distance of 5000 m.

5. Conclusions

In this investigation, Al/SiC/Gr hybrid composites were successfully fabricated using the powder metallurgy route. The hardness and density of the hybrid composites decreased with an increase in graphite content. The composites with 5 wt% Gr exhibited both excellent wear resistance and friction coefficients. The addition of solid lubricant particles as the second reinforcement in the aluminium matrix effectively improves friction and wear properties.

ANOVA showed that the most significant variables affecting the sliding wear of the composites (in terms of their individual percentage contributions) were the sliding distance (57.12%), sliding speed (12.43%), applied load

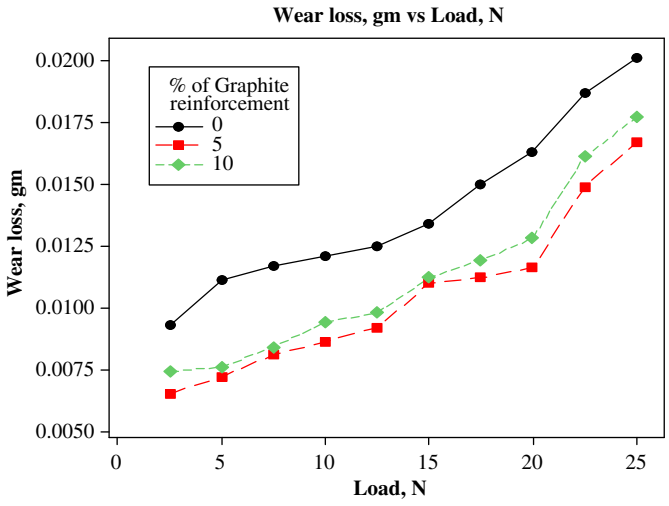

Fig. 14. Variation of wear loss with applied load at a sliding speed of 3 m/s for a sliding distance of 5000 m.

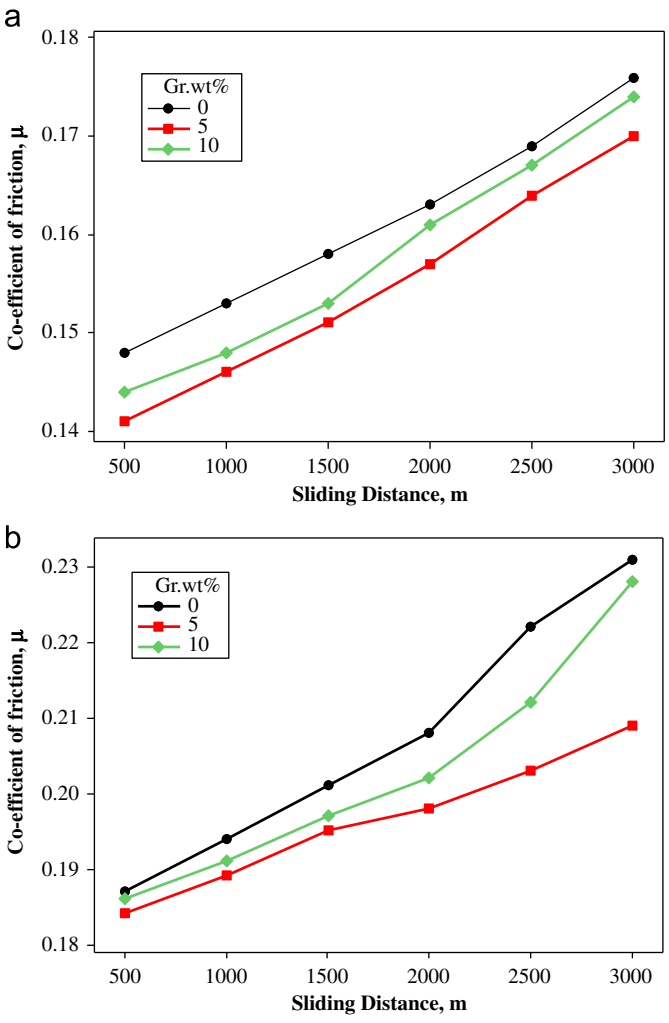

Fig. 15. Variation of co-efficient of friction (a) at applied load of 10 N and (b) at applied load of 20 N.

(13.78%), and graphite content in the composite (11.23%) within the selected range of investigations. ANOVA also showed that the most significant variables affecting the friction behaviour of the composites (in terms of their individual percentage contributions) were the applied load (61.47%), sliding distance (0.86%), sliding speed (8.86%), graphite content in the composite (8.84%) and the interaction effect of the reinforcement and the load (7.73%). The optimal control factors were determined in a Taguchi experimental analysis and found to be A2B1C1D3 for wear loss and A2B1C1D1 for the friction coefficient. The prominent testing parameter for the wear of the composites was found to be the sliding distance. However, the applied load, sliding speed and weight fraction of graphite had only a slight influence on wear loss, while the applied load was found to significantly affect the friction coefficient of the composites.

SEM studies of the worn surfaces and wear debris revealed that the wear mechanism involved with the Al–5% SiC composites was oxidative wear with severe plastic deformation. The wear mechanism with the Al–5% SiC–10% hybrid composites was oxidative wear with delamination wear. With the Al/5% SiC/5% Gr hybrid composites, delamination wear was the prominent wear mechanism. A uniform graphite film on top of the worn surface helped to decrease both the wear loss and friction coefficient. Therefore, severe wear was avoided with the Al/5% SiC/5% Gr composites. The morphology and size of wear debris was dictated by the amount of Gr content in the composite.

References

[1] P. Ravindran, K. Manisekar, P. Narayanasamy, N. Selvakumar, R. Narayanasamy, Application of factorial techniques to study the wear behaviour of Al hybrid composites with graphite addition, Materials and Design 39 (2012) 42–54.

[2] S. Suresha, B.K. Sridhara, Wear characteristics of hybrid aluminium matrix composites reinforced with graphite and silicon carbide particulates, Composites Science and Technology 70 (2010) 1652–1659.

[3] K. Laden, J.D. Guerin, M. Watremez, J.P. Bricout, Frictional characteristics of Al–SiC composite brake discs, Tribology Letters 8 (2000) 237–247.

[4] Dongmei Xuan Zhou, Qiao Zhu, Fa Luo Xie, Zhou Wancheng, Friction and wear properties of C/C–SiC braking composites, Ceramics International 38 (2012) 2467–2473.

[5] Y.Q. Wang, A.M. Afsar, J.H. Jang, K.S. Han, J.I. Song, Room temperature dry and lubricant wear behaviors of Al_2O_3f/SiCp/Al hybrid metal matrix composites, Wear 268 (2010) 863–870.

[6] S. Mahdavi, F. Akhlaghi, Effect of SiC content on the processing, compaction behavior, and properties of Al6061/SiC/Gr hybrid composites, Materials Science 46 (2011) 1502–1511.

[7] S. Basavarajappa, G. Chandramohan, J.Paulo Davim, Some studies on drilling of hybrid metal matrix composites based on Taguchi techniques, Journal of Materials Processing Technology 196 (2008) 332–338.

[8] L. Krishnamurthy, B.K. Sridhara, D. Abdul Budan, Comparative study on the machinability aspects of aluminium silicon carbide and aluminium graphite composite, Materials and Manufacturing Processes 22 (2007) 903–908.

[9] S. Basavarajappa, G. Chandramohan, K. Mukund, M. Ashwin, M. Prabu, Dry sliding wear behavior of Al 2219/SiCp–Gr hybrid metal matrix composites, Materials Engineering and Performance 15 (2006) 668–674.

[10] M.L. TedGuo, C.Y.A. Tsao, Tribological behavior of self-lubricating aluminium/SiC/graphite hybrid composites synthesized by the semi-solid powder-densification method, Composites Science and Technology 60 (2000) 65–74.
[11] Y.Q. Wang, A.M. Afsar, J.H. Jang, K.S. Han, J.I. Song, Room temperature dry and lubricant wear behaviors of Al_2O_3/SiCp/Al hybrid metal matrix composites, Wear 268 (2010) 863–870.
[12] S. Suresha, B.K. Sridhara, Effect of addition of graphite particulates on the wear behaviour in aluminium–silicon carbide–graphite composites, Mater and Design 31 (2010) 1804–1812.
[13] Gaohui Jinfeng Leng, Qingbo Wu, Zuoyong Zhou, XiaoLi Huang Doua, Mechanical properties of SiC/Gr/Al composites fabricated by squeeze casting technology, Scripta Materialia 59 (2008) 619–622.
[14] S. Mahdavi, F. Akhlaghi, Effect of the graphite content on the tribological behavior of Al/Gr and Al/30SiC/Gr composites processed by in-situ powder metallurgy (IPM) method, Tribology Letters 44 (2011) 1–12.
[15] S. Santhosh Kumar, M. Devaiah, V. Seshu Bai, T. Rajasekharan, Mechanical properties of SiCp/Al_2O ceramic matrix composites prepared by directed oxidation of an aluminum alloy, Ceramics International 38 (2012) 1139–1147.
[16] Mohsen Ostad Shabani, Ali Mazahery, Optimization of process conditions in casting aluminum matrix composites via interconnection of artificial neurons and progressive solutions, Ceramics International 38 (2012) 4541–4547.
[17] J. Zhang, R.J. Perez, E.J. Lavernia, Effect of SiC and graphite particulates on the damping behavior of metal matrix composites, Acta Metallurgica et Materialia 42 (1994) 395–409.
[18] K. Yamagushi, N. Takakura, S. Imatani, Compaction and sintering characteristics of composite metal powder, Journal of Materials Processing Technology 63 (1997) 346–350.
[19] ASTM G99–05, Standard Test Method for Wear Testing With a pin-on-disc Apparatus, American Society for Testing and Materials (reapproved 2010).
[20] Prasanta Sahoo, Sujan Kumar Pal, Tribological performance optimization of electroless Ni–P coatings using the Taguchi method and grey relational analysis, Tribology Letters 28 (2007) 191–201.
[21] Minitab User Manual, Making Data Analysis Easier, Release 14, MINITAB Inc., 2001.
[22] C. Douglas, Montgomery, Design and Analysis of Experiments, Wiley India (P) Ltd., 2007.
[23] S. Basavarajappa, G. Chandramohan, A. Mahadevan, Influence of sliding speed on the dry sliding wear behaviour and the subsurface deformation on hybrid metal matrix composite, Wear 262 (2007) 1007–1012.
[24] B. Venkataraman, G. Sundararajan, Correlation between the characteristics of the mechanically mixed layer and wear behaviour of aluminium, Al-7075 alloy and Al-MMCs, Wear 245 (2000) 22–38.
[25] R.K. Gautam, S. Ray, Satish C. Sharma, S.C. Jain, R. Tyagi, Dry sliding wear behavior of hot forged and annealed Cu–Cr–graphite in-situ composites, Wear 271 (2011) 658–664.
[26] T. Savaskan, O. Bican, Dry sliding friction and wear properties of Al–25Zn–3Cu–(0–5) Si alloys in the as-cast and heat-treated conditions, Tribology Letters 40 (2010) 327–336.
[27] S. Rajkumar, Aravindan, tribological performance of microwave sintered copper–TiC–graphite hybrid composites, Tribology International 44 (2011) 347–358.
[28] Y. Sahin, V. Kilicli, Abrasive wear behaviour of SiCp/Al alloy composite in comparison with ausferritic ductile iron, Wear 271 (2011) 2766–2774.
[29] Wenlin Ma, Jinjun Lu, Effect of surface texture on transfer layer formation and tribological behaviour of copper–graphite composite, Wear 270 (2011) 218–229.
[30] E. Mohammad Sharifi, F. Karimzadeh, Wear behavior of aluminum matrix hybrid nano composites fabricated by powder metallurgy, Wear 271 (2011) 1072–1079.
[31] Xiaomeng Fan, Xiaowei Yin Shanshan He, Litong Zhang, Laifei Cheng, Friction and wear behaviors of C/C–SiC composites containing Ti_3SiC_2, Wear 274–275 (2012) 188–195.
[32] C.S. Ramesh, R. Keshavamurthy, G.J. Naveen, Effect of extrusion ratio on wear behaviour of hot extruded Al6061–SiC(Ni–P coated) composites, Wear 271 (2011) 1868–1877.
[33] B.V.Manoj Kumar, Young-Wook Kim, Dae-Soon Lim, Seo Won-Seon, Influence of small amount of sintering additives on unlubricated sliding wear properties of SiC ceramics, Ceramics International 37 (2011) 3599–3608.
[34] Jianxin Deng, Tongkun Can, Junlong Sun, Microstructure and mechanical properties of hot-pressed Al/TiC ceramic composites with the additions of solid lubricants, Ceramics International 31 (2005) 249–256.
[35] Ali Mazahery, Mohsen Ostad Shabani, Study on microstructure and abrasive wear behavior of sintered Al matrix composites, Ceramics International 38 (2012) 4263–4269.